Journal of the European Ceramic Society 20 (2000) 967–976

An investigation of conductivity, microstructure and stability of HfO_2–ZrO_2–Y_2O_3–Al_2O_3 electrolyte compositions for high-temperature oxygen measurement

Serge Zhuiykov*

Analyt Instruments, 15/594 Inkerman Road, Caulfield North, VIC. 3161, Australia

Received 22 April 1999; received in revised form 3 August 1999; accepted 12 August 1999

Abstract

In search of better ionically conducting ceramics for high temperature oxygen fuel cells and sensors, the conductivity and microstructure of the HfO_2–ZrO_2–Y_2O_3 system with 15 mol% of Y_2O_3 and the HfO_2–ZrO_2–Y_2O_3–Al_2O_3 system with 50 mol% of Al_2O_3 have been investigated with X-ray diffractometry (XRD), scanning electron microscopy (SEM) and conductivity measurements as a function of temperature. The stability of electrolyte compositions was studied by continuously monitoring conductivity as a function of time at 1000°C. A majority of the investigated samples exhibited linear Arrhenius plots of the lattice conductivity as a function of temperature. In the HfO_2–ZrO_2–Y_2O_3–Al_2O_3 electrolyte systems the parameter pe' was measured at a temperature range of 1000–1400°C. The HfO_2–ZrO_2–Y_2O_3–Al_2O_3 electrolyte systems have also showed better thermal shock resistance than the ZrO_2–Y_2O_3 systems. A comparison between the ageing of ZrO_2- and HfO_2-based electrolyte systems, as a result of long time annealing at a temperature of 1000°C, indicated that the degradation of the HfO_2-based system at a temperature of 1000°C and above is 1.5 times lower than the degradation of the ZrO_2-based systems. © 2000 Elsevier Science Ltd. All rights reserved.

Keywords: Al_2O_3; Composites; Ionic conductivity; Microstructure-final; Sensors; Thermal shock resistance; ZrO_2

1. Introduction

Research into new ionic conductors based on the stabilised zirconia (ZrO_2) systems has reached a level of maturity where most studies on such materials concentrate mainly on obtaining incremental improvements in conductivity by better processing control and refinement of the microstructure. Further increases in the conductivity are important in terms of enhancing the efficiency of systems such as oxygen sensors, high temperature fuel cells, electrochemical oxygen pumps and heating elements.[1–5] Considerable research has been devoted to the understanding of the influence of various stabilising oxides on the ionic conductivity and the defect structure of solid electrolytes.[6–8] However, much less attention has been given to the investigations of the hafnia (HfO_2) and HfO_2–ZrO_2-based solid electrolytes. This could be explained by the fact that HfO_2 is considerably more expensive than ZrO_2, which makes it less attractive for practical applications.

The obtained experimental studies of the ionic conductivities of doped HfO_2 solid electrolytes at temperatures of 700–1000°C have been rare and differ significantly.[7–11] Most of the work involving HfO_2 and stabilising oxides has addressed only to the structure and assessment of new phase diagrams from X-ray diffractometry (XRD). However, very little has been done towards the searching of the HfO_2–ZrO_2 electrolyte systems in regard to optimise the ionic conductivity at high temperatures up to 1600°C, good thermal shock resistance and low permeability.[9] Moreover, no extensive studies have been available on the ionic and electronic conductivities of HfO_2-based electrolytes at high temperatures up to 1600°C. The HfO_2–ZrO_2–Y_2O_3 system is complex and the true equilibrium phase diagram has still not been fully resolved. The limits of applicability of ZrO_2 electrolytes featuring a cubic fluorite-type of structure, especially at temperatures higher than 1100°C, are determined by partial electronic conductivity, which increases as oxygen partial pressure (Po_2) decreases down to the level of 10^{-23}–10^{-28} Pa. Partial electronic conductivity permits an oxygen-ion

---

* *E-mail address*: sz98uk@hotmail.com

PII: S0955-2219(99)00233-2

flux across the electrolyte and causes electromotive force (EMF) mismeasurement due to the interfacial polarisation.[9] ZrO_2 also may be chemically reduced at low Po_2 levels. One possible way to minimise this short-circuit electronic conductivity is to use fully-stabilised zirconia.[10] However, the fully-stabilised zirconia possesses a substantially lower level of ionic conductivity than the partially-stabilised one. [3] Thus, the development of alternative ion-conducting materials, such as HfO_2–ZrO_2-based electrolytes for thermodynamic control of oxygen impurity in high-melting metals and alloys in non-ferrous metallurgy, semiconductor industry and for the copper refineries is required. Such application environments are characterised both very high temperatures and extremely low oxygen potential. Good thermal shock resistance and inertness to chemical attack by electrode materials are some of the other properties needed for application within certain ranges of temperature and oxygen pressure.

The physicochemical and thermomechanical properties of selected pure oxides are summarised in Table 1. Studies regarding ternary phase diagrams were reported on the HfO_2–ZrO_2–Y_2O_3 system (Fig. 1).[3] The previous research[7] shown that the pure cubic HfO_2 electrolyte with 8–12 mol% of Y_2O_3 has no significant advantage over the ZrO_2–Y_2O_3 electrolyte with the same dopant concentration in terms of high ionic conductivity at the temperature range of 700–1000°C. Furthermore, the ionic conductivity of HfO_2–Y_2O_3 system (10 mol% of Y_2O_3) was found even lower than the conductivity of ZrO_2–Y_2O_3 system (10 mol% of Y_2O_3) in above-mentioned temperature range.[7] However, in comparison with ZrO_2, the HfO_2 solid electrolyte features a higher chemical stability, higher resistivity to rapid temperature changes and much less electronic conductivity at temperatures over 1200°C.[10]

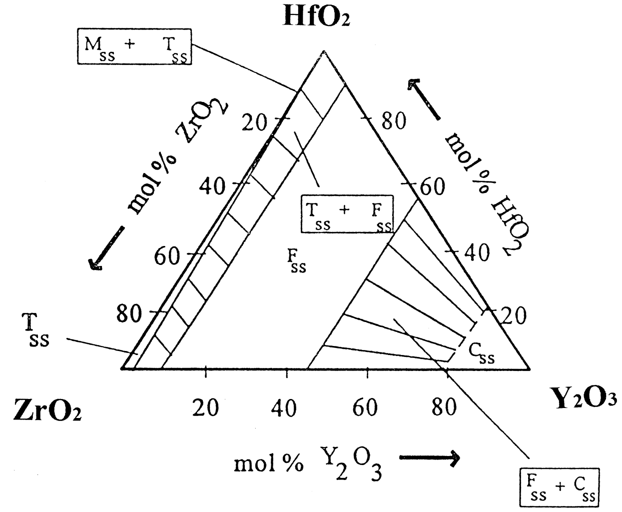

Fig. 1. Ternary phase diagram HfO_2–ZrO_2–Y_2O_3 at 1600°C.

The presence of alumina in ZrO_2 electrolyte leads to higher resistance against thermal stresses.[12] α-Alumina exhibits the absence of chemical reactions in ZrO_2–Y_2O_3 systems, lower coefficient of thermal expansion and higher heat conductivity than zirconia. As a consequence of this, alumina could not only improve the thermomechanical properties of stabilised HfO_2–ZrO_2 composites but also could play a decisive role in the heterojunction between the HfO_2–ZrO_2 electrolyte and an Al_2O_3 insulator in practical designs of the oxygen sensors. Further complicating factor that has been observed in the traditional zirconia systems is the effect of high temperature (~1000°C) annealing on the deterioration of conductivity of the ZrO_2 electrolyte. This ageing process could certainly be reduced by the addition of Y_2O_3. However, the electrolyte material, in this case, will suffer a consistent decrease in the overall conductivity with increasing Y_2O_3 content. In an attempt to overcome this problem of ageing, different HfO_2–ZrO_2 electrolyte systems should be investigated.

In regard to the aforementioned aspects, the purpose of this study is to investigate microstructure, the ionic and electronic conductivities and stability of alternative composite HfO_2–ZrO_2 electrolyte system for oxygen measurements at high temperatures and low oxygen partial pressures, and to compare the results with other presently known ZrO_2 electrolyte systems.

Table 1

Property	ZrO_2	HfO_2	Y_2O_3
Structure	Monoclinic	Monoclinic	Cubic
Transition temperature (°C)	1205	1700	–
Monoclinic↔tetragonal			
Tetragonal↔cubic	2370	2700	–
Cubic↔tetragonal	–	–	2350
Melting point (°C)	2677	2900	2420
Boiling point (°C)	4300	–	–
Density at 20°C (g/cm^3)	6.1	9.68	5.03
Coefficient of the thermal expansion , α, at 1000°C ($\times 10^{-6}$ K^{-1})	7.01	5.3	8.3
Specific electrical conductivity, k, at 1000°C [(Ωcm)$^{-1}$]	10^{-2}	–	–
Thermal conductivity, λ, at 100°C [W(mK)$^{-1}$]	1.67–2.09	–	14

2. Experimental procedure

2.1. Samples preparation

Samples were prepared by mixing 99.95% pure HfO_2, 99.95% pure ZrO_2, 99.99% pure Y_2O_3 and 99.9% pure Al_2O_3 (Aldrich Chemicals Pty. Ltd., Australia). The components were weighed and mixed manually with acetone in an agate mortar or automatically in mixer for ~50 h. The mixtures were dried and then pressed and calcined at 1300°C for 18 h. For the samples of the HfO_2–ZrO_2–Y_2O_3 system, where the composition was 65–20–15 mol%, the presintered pellets were crushed in an agate mortar and then powders obtained were rubber-pressed into pellets and sintered at 1650°C for 6 h in air. For the samples of the HfO_2–ZrO_2–Y_2O_3–Al_2O_3 system, where Al_2O_3 was 50 mol%, the presintered pellets of HfO_2–ZrO_2–Y_2O_3 were crushed in an agate mortar, certain amount of Al_2O_3 was added and mixed and then powders obtained were also rubber-pressed into pellets and sintered at 1700°C for 5 h in air. The sintered pellets were cut into pieces of about 4 mm in diameter and less than 5 mm in length and some of them were welded into Al_2O_3 insulating tubes, as shown in Fig. 2. The cylinder-tube design is a robust form of construction of the sensor and avoids any possible leaks through the junction of the solid electrolyte and insulating tube. The amount of Al_2O_3 was calculated to avoid significant anisotropy in the coefficients of thermal expansion of both solid electrolyte pellets and alumina tube. The Pt electrodes were painted onto both faces of the electrolyte samples and sintered on at 900°C in air for 120 min. The sensors were checked for a leakage at room temperature before they were sealed. Measurements were made using both an increasing and decreasing temperature cycle to ensure the results were consistent. A built-in R-type thermocouple was used. The EMF was measured with a high impedance digital multimeter 179 TRMS accurate to ±0.1 mV.

Fig. 2. Designs of the HfO_2–ZrO_2-based oxygen sensor for different applications.

2.2. Phase analysis and lattice parameter measurements

Routine phase identification of the HfO_2–ZrO_2–Y_2O_3 samples was performed using a Rigaku X-ray diffractometer with Ni-filtered CuK_α radiation. The experimental conditions were: scan range from 5 to 80°, scan speed 1° and step size 0.05°. All investigated samples were single phase with fluorite-type structure. Lattice parameters were calculated using the *d*-spacing values from XRD. For calculation, a well-known equations in standard textbooks were used. The refinement of unit-cell parameters was done with a computer program. The effective precision of the measurements was ±0.0005 nm.

Analytical electron microscopy was also performed on selected HfO_2–ZrO_2–Y_2O_3–Al_2O_3 specimens to determine the phase assemblage and composition. Samples were polished by using Metadi II-diamond polishing compound (USA) and were coated with a 30 nm coating of carbon. The microscopy was performed using a JEOL JSM-6440F filed emission scanning electron microscope fitted with both digital imaging system for electron microscope and energy dispersive X-ray detector VOYAGER (USA).

Four-probe d.c. conductivity measurements were performed at a range of temperature between 700 and 1000°C. To investigate the ageing behaviour, specimens were maintained at 1000°C for 42 days (1000 h) and conductivity measurements were made over this time span.

2.3. Ionic conductivity and pe′ parameter measurements

The faces of the sintered pellets were polished to a 1-μm surface finish using Metadi II-diamond polishing compound (USA). Pt electrodes were applied by painting on a Pt paste (Engelhard Pty. Ltd., Australia). The specimens were suspended in the center of the hot zone of a furnace. Temperature was measured using R-type of thermocouples positioned at $\leqslant 1$ mm from the sample. The temperature was controlled within ±1°C. The complex impedance analysis technique was employed. The measured impedance values were corrected for the resistance and inductance of the platinum leads prior to further analysis.

In the present study a known thermodynamic EMF method was applied to determine the parameter pe'. This parameter pe' describes the relation between the partial ionic and *n*-type electronic conductivity of the electrolyte and is defined as the P_{o2} at which the ionic conductivity and the *n*-type electronic conductivity of the electrolyte are equal. Basically, it is accepted that this parameter must be consistent and known to a high degree of accuracy if precise and useful measurements are to be made. This method has already been described comprehensively in previous publications. [13,14] When HfO_2–ZrO_2 electrolyte systems are exposed to the high temperatures ($T > 1100°C$) and low oxygen partial pressures ($P_{o2} < 10^{-20}$ Pa) they exhibit mixed ionic and *n*-type electronic conductivities. Under these conditions, the electrochemical device generates an EMF that is influenced by the electrical properties of solid electrolyte. Schmalzried[15] has analysed the contribution of electronic conductivity in the zirconia solid electrolyte to the measured EMF of an electrochemical cell in the P_{o2} region less than 10^5 Pa and has shown that, in the presence of *n*-type electronic conductivity, the EMF (E) of the electrochemical cell could be expressed as:

$$E = \frac{RT}{4F}\int_{P_{o2(I)}}^{P_{o2}(II)} t_{ion} d(\ln P_{o2}) = \frac{RT}{F}\ln\frac{pe'^{1/4} + P_{o2}(II)^{1/4}}{pe'^{1/4} + P_{o2}(I)^{1/4}}, \quad (1)$$

where $P_{o2}(II)$ and $P_{o2}(I)$ are the respective oxygen partial pressures at the two electrolyte-electrode interfaces, R is the gas constant, F is the Faraday constant, and T is the absolute temperature. To satisfy the condition $P_{o2}(II) >> pe' > P_{o2}(I)$,[13] an Al melt contained in an alumina crucible was used to represent the extremely low oxygen partial pressure $P_{o2}(I)$. Aluminium was selected from the group of high-melting metals because it has a lowest oxygen potential at temperature of 700°C and higher.[16] Since the work of Schmalzried, several investigators[10,13] have analysed and emphasised the importance of an accurate knowledge of the value of the parameter pe' specifically for measurement of low oxygen partial pressure by the ZrO_2 sensors.

The EMF measurements were made using sensors (Fig. 2) consisting of the HfO_2–ZrO_2–Y_2O_3–Al_2O_3 electrolyte system and an inner Cr–Cr_2O_3 reference electrode. Similar sensors based on the ZrO_2–Y_2O_3 electrolyte with 10 mol% of Y_2O_3 were used for comparison. Both types of sensors were immersed into the melt at a temperature range of 1000–1400°C. Stable EMF recordings were obtained after 7–9 min. These EMF values were then used to calculate the pe' values by rearranging Eq. (1), as follows:

$$pe' = \frac{\left\{\left[\exp\left(\frac{EF}{RT}\right)\right]P_{o2}(I)^{1/4}\right\} - P_{o2}(II)^{1/4}}{1 - \exp\left(\frac{EF}{RT}\right)}. \quad (2)$$

Low values of the parameter pe' (ionic transference number, t_{ion}, is 0.5) indicate low contributions of partial electronic conductivity to the total conductivity, which results in higher ionic conductivities (k) according to the equation

$$k_{ion} = Kpe',^{-1/4} \quad (3)$$

where K is a constant and $P_{o2} = pe'$ and $ke' = k_{ion}$ at $t_{ion} = 0.5$. By knowing pe', it is possible to calculate t_{ion} as a function of P_{o2} using the expression

$$t_{ion} = \left[1 + \left(\frac{P_{02}}{pe'}\right)^{-1/4}\right]^{-1}. \quad (4)$$

3. Results and discussion

Fig. 3 shows the XRD trace of the sample of HfO_2–ZrO_2 electrolyte doped with 15 mol% Y_2O_3, from which the predominance of cubic hafnia-zirconia phase was identified. This solid electrolyte system was selected for the investigation due to its lowest level of the pe' parameter at high temperatures as it was clearly shown in Fig. 4.[9] The lattice parameter of the cubic phase was calculated ($a = 5.138$ Å) and it was in good agreement with those lattice parameters of the same solid electrolyte system which were reported by other authors ($a = 5.137$ Å) [9] and ($a = 5.138$ Å).[7] However, obtained data were in the satisfactory agreement with the results of other investigators ($a = 5.152$ Å).[5] When the intensity scale of the XRD peaks was enlarged, a shoulder was found at the peak of $2\theta = 62.3°$ and a fine splitting of the peak at $2\theta = 73.4°$ was also observed. It is suggested that the two peaks may correspond to the (004) and (400, 040) peaks for the tetragonal zirconia phase. However, the intensity ratio of these two peaks is reversal of that for a single tetragonal phase. Therefore, this result appears to indicate a mixture of cubic hafnia and zirconia and tetragonal zirconia phases with cubic form as the dominant one. A tetragonal zirconia cell was subsequently calculated, based on the (400) split peaks, giving the result of $a = 5.132$ Å and $c = 5.140$ Å. In addition to the hafnia and zirconia phases few peaks with very weak intensities were also observed in the XRD trace (e.g. $d = 3.31$ Å and $d = 2.02$ Å in Fig. 3). Due to low intensity of these peaks, they have not been positively identified.

The microstructure of HfO_2–ZrO_2–Y_2O_3–Al_2O_3 composite solid electrolytes is shown in Fig. 5. The dark areas are the Al_2O_3 phase and the white areas are the HfO_2–ZrO_2–Y_2O_3 phase. The radius of both Al_2O_3 and HfO_2–ZrO_2 grains in this structure is various from 5 to 15 μm. However, in average, the hafnia-zirconia grains are bigger than the alumina grains. This appear to indicate that this structure may be the most preferred for optimisation of the conductivity and in terms of the microhardness values and fracture toughness of the

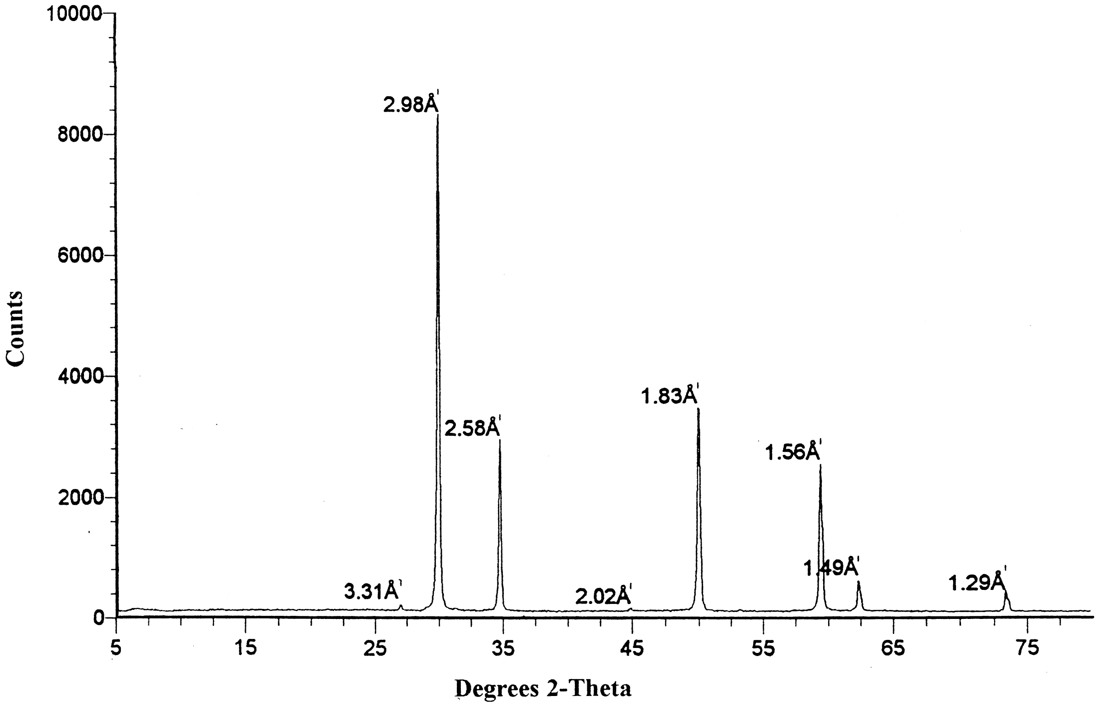

Fig. 3. X-ray powder diffraction patterns of HfO_2–ZrO_2–Y_2O_3 solid electrolyte system showing the presence of mainly a cubic phase.

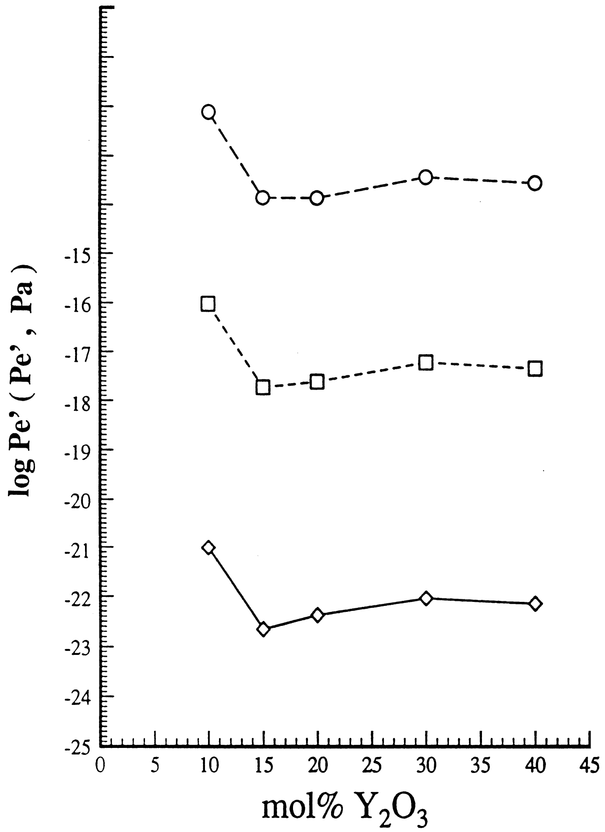

Fig. 4. Plot of log *pe'* vs mol% Y_2O_3 for HfO_2–ZrO_2-based system, using the thermodynamic EMF method and plug-type sensor (◇, 1200°C; □, 1400°C; ○, 1600°C).

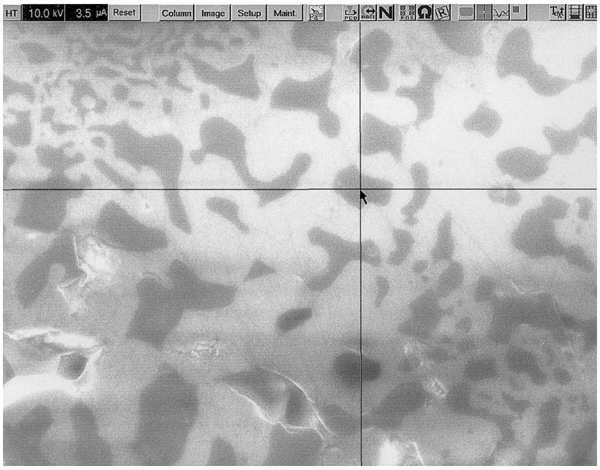

Fig. 5. Typical structure of transverse section of HfO_2–ZrO_2–Y_2O_3–Al_2O_3 composite shown by field emission scanning electron microscopy (SEM). The dark phase is Al_2O_3; the light phase is HfO_2–ZrO_2.

composite systems. Investigations of the phase assemblage of the HfO_2–ZrO_2–Y_2O_3–Al_2O_3 electrolyte systems show the presence mainly of two phase, one of which is the phase with the cubic fluorite-type structure of the HfO_2–ZrO_2–Y_2O_3 composition [Fig. 6(a)]. Another phase is alumina [Fig. 6(b)].

The values of the parameter *pe'* were measured as a function of temperature for both HfO_2–ZrO_2–Y_2O_3–Al_2O_3 and HfO_2–ZrO_2–Y_2O_3 electrolyte systems. The thermodynamic EMF method with plug-type sensors

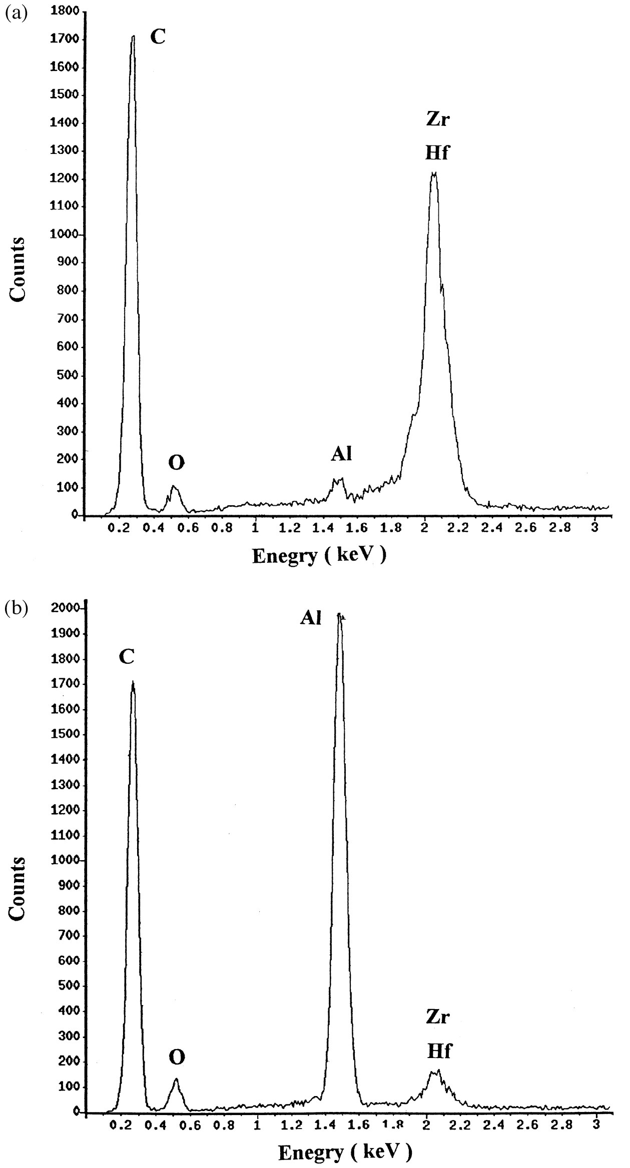

Fig. 6. Energy dispersive X-ray trace of a region of the HfO_2–ZrO_2–Y_2O_3–Al_2O_3 electrolyte structure: (a) within the grain of the stabilised HfO_2–ZrO_2; (b) within the grain of Al_2O_3.

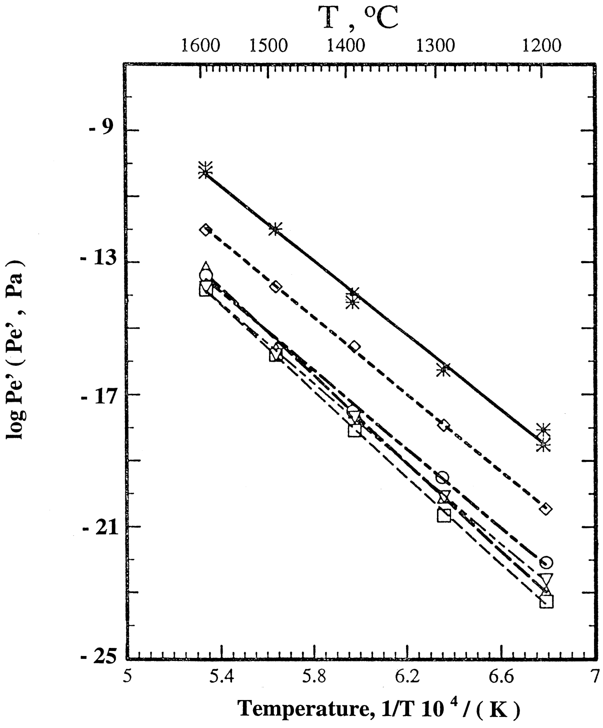

Fig. 7. Plot of log pe' vs $1/T$ functions for selected binary and ternary HfO_2- and ZrO_2-based solid electrolytes in plug-type sensors: (*) - ZrO_2–15 mol% CaO;[9] ◇, ZrO_2–10 mol% Y_2O_3; △, HfO_2–15 mol% Y_2O_3;[9] ○, HfO_2–ZrO_2–Al_2O_3–15 mol% Y_2O_3; □, HfO_2–ZrO_2–15 mol% Y_2O_3.

(Fig. 2) has been used in these measurements. The results of these measurements were shown in Fig. 7. Additional data, reported by other investigations, [9] were presented for comparison. As demonstrated earlier in Fig. 4, a minimum parameter pe' value was observed at ~15 mol% Y_2O_3 in the entire temperature range, which was in good agreement with the previously published data for high temperature range of 1200–1600°C.[9] Some discrepancies are obvious at lower temperatures due to a distortion of the microstructure caused by the sluggish reactions in ceramic systems. It is possible that an addition sintering effect during the immersion of the sensors into the melt was occurred and it was responsible for more precise values of the pe' parameter. Although the shapes of the curves for the HfO_2–ZrO_2–Y_2O_3–Al_2O_3 and HfO_2–ZrO_2–Y_2O_3 systems were similar to the shapes of the curves for the ZrO_2–Y_2O_3 system, the measured values of the parameter pe' for the ZrO_2–Y_2O_3 system were considerably lower than for the HfO_2–ZrO_2–Y_2O_3 system. This suggests that the HfO_2-based solid solutions exhibit considerably lower parameter pe' values (lower partial electronic conductivity) than the ZrO_2-based solid solutions. Generally, the ionic conductivity is governed by the diffusion of oxygen ions across oxygen-ion vacancies. Up to certain doping content, the mobility of charge carriers is due to O^{2-} ion vacancies. However, the mobility of the vacancies will be diminished if the doping content will be increased. At high concentrations of stabilised oxide there is a large probability that a given anionic site becomes the neighbour of two or more dopant cations. These sites then act as deep traps for oxygen vacancies. Deep trapping would certainly contribute to the rapid decrease in conductivity beyond its maximum. Therefore, an addition increase of the Y_2O_3 content in the solid electrolyte system did not shift towards a lower partial electronic conductivity. The changing in ionic conductivity for HfO_2–Y_2O_3 system is depending on the doping concentration and it is shown in Fig. 8 for the temperature of 800°C.[7] The curve has a similar shape for higher temperatures. The data presented in this figure clearly show that the ionic conductivity of HfO_2-based systems decreases as a doping concentration increases from 10 mol%. It is also interesting to note that the maximum conductivity of the HfO_2–Y_2O_3 system was obtained at 10 mol% of Y_2O_3.[7] In addition, the minimum *pe′* parameter for HfO_2–ZrO_2–Y_2O_3 system was found at 15 mol%. It is, therefore, apparent that the optimum percentage of Y_2O_3 should be within the range of 10–15 mol% for practical sensor applications.

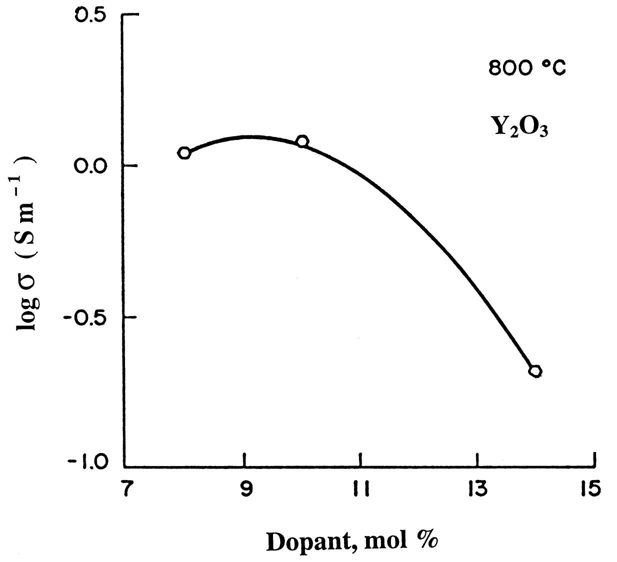

Fig. 8. Ionic conductivity measured at 800°C as a function of dopant concentration for Y_2O_3-doped HfO_2.

The Arrhenius plot of HfO_2- and ZrO_2-based electrolyte samples free of Al_2O_3 additions are shown in Fig 9. Both compositions showed a change in slope of the Arrhenius plots similar to that reported previously by a number of other authors.[3,7,9] The measurements of ionic conductivities were done at one frequency using four probe method where the influence of grain boundary resistance was not accounted for. Fig. 9 shows that at the temperatures lower than 1000°C the ionic conductivities of zirconia electrolyte system are slightly higher and activation enthalpy lower than for the hafnia electrolyte system. However, at the temperature more than 1000°C the difference in ionic conductivities became negligible and at the temperature over 1300°C the HfO_2-based electrolyte system have higher ionic conductivities than the ZrO_2-based electrolyte system. It is very clear from the consistency of the results when using increasing and decreasing temperature cycles that the measurements at each temperature are repeatable.

Fig. 10 illustrates the ionic transference number (t_{ion}) as a function of P_{o2} in the range of ~1–10^{-25} Pa for HfO_2–ZrO_2–Y_2O_3 and other selected HfO_2-based systems[9] at 1600°C. These results appear to indicate that the HfO_2-based electrolyte systems are preferable for use in the applications where both high temperatures and low oxygen partial pressures are combined. Under certain circumstances, the partial electronic conductivity of those electrolytes is negligible, as compared to ionic conductivity at these extreme conditions. These values are essential for the further development of the solid electrolyte oxygen

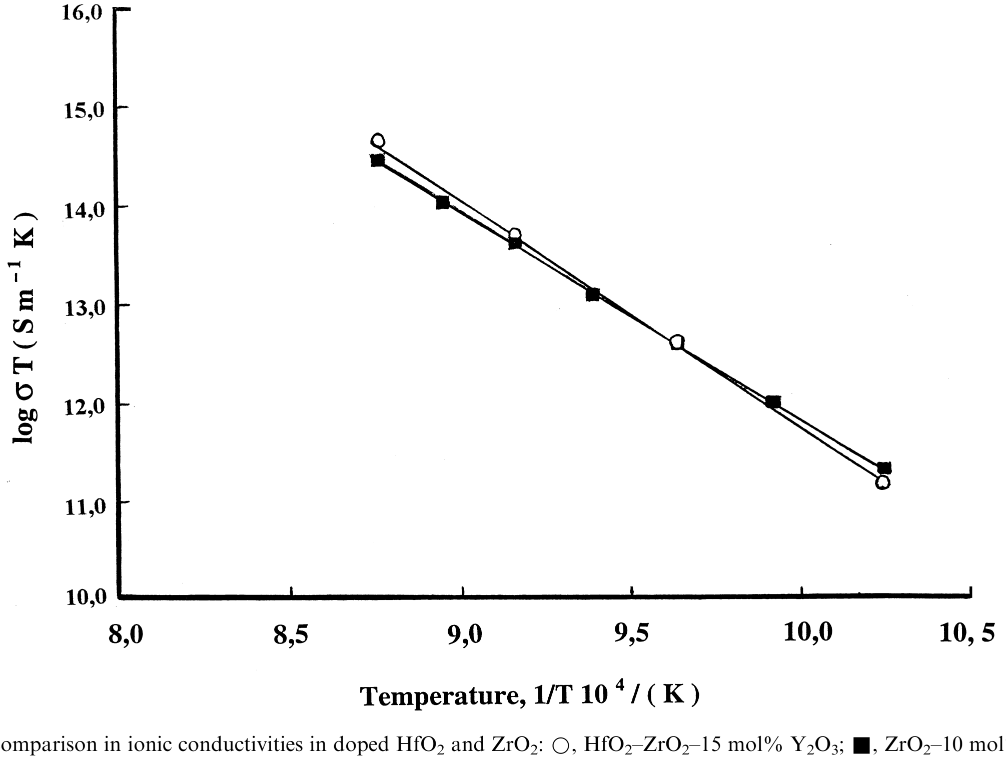

Fig. 9. Comparison in ionic conductivities in doped HfO_2 and ZrO_2: ○, HfO_2–ZrO_2–15 mol% Y_2O_3; ■, ZrO_2–10 mol% Y_2O_3.

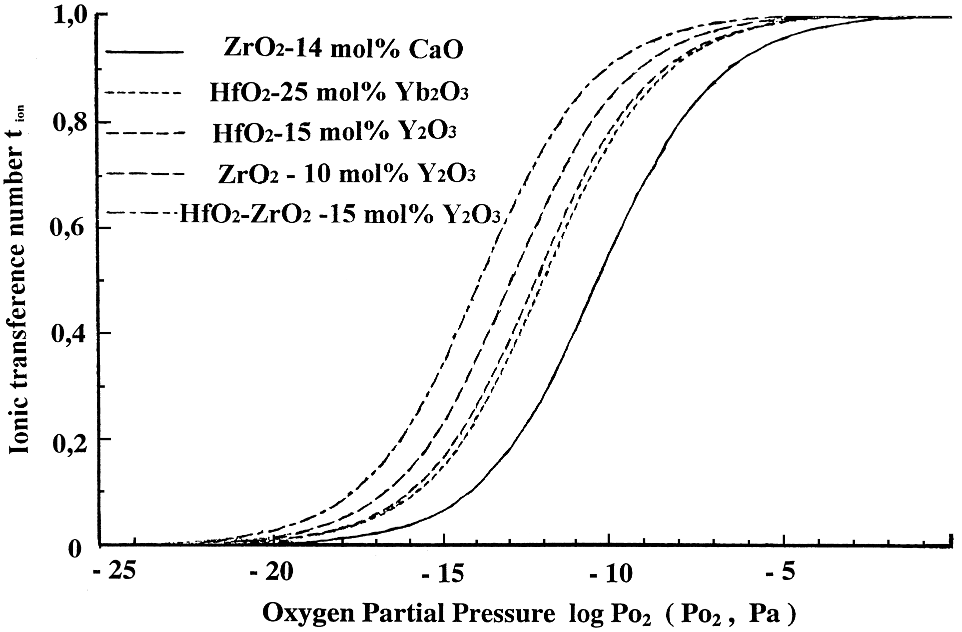

Fig. 10. Ionic transference number (t_{ion}) as a function of oxygen partial pressure P_{o2} at 1600°C for selected HfO_2-based solid electrolytes: ZrO_2–14 mol% CaO; HfO_2–25 mol% Yb_2O_3; HfO_2–15 mol% Y_2O_3; HfO_2–ZrO_2–15 mol% Y_2O_3.

sensors with respect to the conditions encountered in fully killed steel melts ($T = 1400-1700$°C; $P_{o2} = 10^{-9}-10^{-12}$ Pa). The partial electronic conductivities for HfO_2–ZrO_2–Y_2O_3 electrolyte were more than two orders of magnitude less than the partial electronic conductivities for ZrO_2–Y_2O_3 electrolyte at 1000–1600°C, as clearly shown in Fig. 7. If well-known ZrO_2–Y_2O_3 electrolyte could be replaced by HfO_2–ZrO_2–Y_2O_3 electrolyte systems are attainable in the practical industrial situations. Thus, the HfO_2-based electrolyte systems are applicable and likely to use at 1200–1600°C when the measuring P_{o2} is $\sim 10^{-13}$ Pa and lower, where the ZrO_2-based electrolytes start to exhibit the *n*-type electronic conductivity. These results also confirmed those of the previous investigations [9] where a higher content of HfO_2 in the ternary solid solutions led to lower parameter pe' values.

From a practical point of view, it is very important to know how the conductivity of solid electrolyte may decrease with time, referred to as ageing as a result of long time annealing at a temperature of ≈1000°C and higher. The ageing of solid electrolyte system has an influence on the major characteristics of the sensor. The accuracy and stability of the sensor may be effected during the high temperature measurements as a result of ageing. The results of experimental investigations of ZrO_2-based solid electrolytes indicate that the ageing kinetic has a different nature for single- and two-phase polycrystalline electrolytes. Moreover, it is also dependent upon which stabilising oxide (Y_2O_3, MgO, Yb_2O_3, Sc_2O_3, etc.) was selected for the preparation of ZrO_2 electrolyte. It is also dependent upon the molar percentage rate between solid electrolyte and stabilising oxide. For example, ZrO_2–Sc_2O_3 electrolytes show higher rate of ageing than ZrO_2–Y_2O_3 electrolytes.[17]

The raise of electrical resistivity of the ZrO_2–Y_2O_3 electrolyte systems is attributed to segregation of an yttria-rich layer near the grain boundaries and triple points *electrode–electrolyte–gas*, formation of tetragonal ZrO_2 at temperature above 900°C and retention of this metastable form along with the stabilised fluorite phase on cooling to lower temperature as well as ordered domains forming within the disordered fluorite phase. In industrial applications the lower the resistivity of the zirconia oxygen probe the greater the electrode contact area in the assembly. For example, a value below 15 kΩ at temperatures above 820°C is acceptable for a ZrO_2 oxygen probe.[18] A higher figure usually indicates a problem. Therefore, the electrical resistivity measurement has been one of the most common methods of probe testing in industry for years.

In our investigation HfO_2–ZrO_2–Y_2O_3 and ZrO_2–Y_2O_3 solid electrolyte specimens with platinum electrodes and with 15 and 10 mol% of Y_2O_3, respective, were annealed for 42 days (1000 h) at 1000°C. It has recently been found[19] that the ageing process does not occur before 1000°C in electrolytes doped with 10 mol% of Y_2O_3. Investigations of ageing processes have shown that a ZrO_2 electrolyte containing 10 mol% of Y_2O_3 is much less affected by the ageing process than the same electrolyte containing 8 mol% of Y_2O_3. With a lower than 10 mol% of Y_2O_3 the cubic solid solution gradually breaks up into two phases, thus leading to a drop in its electrical conductivity. [20] Therefore, ZrO_2 electrolytes containing a 10 mol% of Y_2O_3 have been used in our tests.

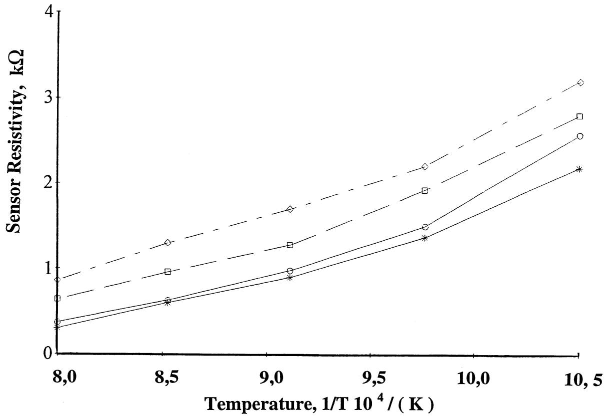

Fig. 11. Measurements of the resistivity of solid electrolyte systems before and after annealing at 1000°C for 1000 h: *, ZrO_2–10 mol% Y_2O_3 before annealing; ○, HfO_2–ZrO_2–15 mol% Y_2O_3 before annealing; ◇, ZrO_2–10 mol% Y_2O_3 after annealing; □, HfO_2-ZrO_2–15 mol% Y_2O_3 after annealing.

Fig. 11 shows the results of the resistivity measurement for both electrolyte specimens before and after annealing. The deterioration of conductivity of ZrO_2–Y_2O_3 sample is significant, however the level of reduction is still such that the total conductivity remains high. It also well-known that the rate of conductivity deterioration of ZrO_2–Y_2O_3 electrolyte compositions is very rapid during the initial stages of the anneal. Nevertheless, it slows down considerably and it appears that the deterioration will settle down after prolonged heat treatment. A number of features of these results require further elaboration. This is a trend in the amount of conductivity reduction with time which is related in some way to the amount of HfO_2 present in the HfO_2–ZrO_2–Y_2O_3 system. The HfO_2–ZrO_2–Y_2O_3 electrolyte showed similar degradation rate in conductivity to the ZrO_2–Y_2O_3 electrolyte as a function of time but the degradation rate decreased with an increase in the HfO_2 content. For example, the resistivity of HfO_2–ZrO_2–Y_2O_3 electrolyte (15 mol% of Y_2O_3 and 65 mol% of HfO_2) at a temperature of 1000°C was increased by ~50% after 42 days of annealing. In contrast, the resistivity of ZrO_2–Y_2O_3 (10 mol% of Y_2O_3) electrolyte at the same temperature was increased by ~110%. This may suggest that the main cause of ageing of solid electrolytes in the two-phase region appears to be the precipitation and growth of the second conductive phase. The kinetic of the ageing process is determined by the kinetic of two processes running independently of each other: growth of the number of second phase centers and the growth of their bulk. In the case of polycrystalline solid electrolytes the process of the second phase growth is connected with the diffusion of solid solution components. Therefore, an increase in the HfO_2 content in the HfO_2–ZrO_2–Y_2O_3 system diminishes the degradation rate in conductivity of composite electrolyte. These results also appear to indicate that the HfO_2-based electrolytes are more likely to be used in sensors measuring extremely low oxygen partial pressure at temperatures higher than 1000–1100°C.

4. Conclusions

All of the investigated HfO_2–ZrO_2–Y_2O_3 electrolyte systems exhibited linear Arrhenius plots of the lattice conductivity as a function of temperature. The difference in ionic conductivities between HfO_2–ZrO_2–Y_2O_3 and ZrO_2–Y_2O_3 solid electrolytes decreases as the temperature rises and at the temperature more than 1300°C the HfO_2-based solid solutions exhibited higher ionic conductivities than the corresponding ZrO_2-based solid solutions. The experimental evaluations of the parameter pe' for HfO_2–ZrO_2–Y_2O_3 showed that the HfO_2-based solid solutions exhibited considerably lower parameter pe' values (by one to two orders of magnitude) than ZrO_2-based solid solutions at high temperature range of 1200–1600°C. Therefore, one of the advantages of the HfO_2-based electrolytes is seen for the sensor applications in the environments where the high temperature (> 1100°C) and extremely low oxygen partial pressures ($P_{o2} = 10^{-12}$–10^{-25} Pa) have been combined. These applications are thermodinamic control of oxygen impurity in high melting metals, alloys, fully killed steel melts, as well as in copper refineries and in carburasing industries. Under above-mentioned working conditions, the HfO_2-based electrolyte systems possess much less electronic conductivity than the ZrO_2-based electrolyte systems.

The results presented here also indicate that the sensors based on HfO_2 electrolyte systems much less affected by the ageing process than the corresponding ZrO_2-based electrolyte systems. Thus, the ageing of the HfO_2-based electrochemical sensor has less influence on its major characteristics such as an accuracy and stability. Furthermore, the HfO_2-based solid solutions have a higher chemical resistivity and thermal shock stability than ZrO_2-based electrolytes. As a consequence of this, they may be recommended as an alternative solid electrolytes for use in sensors measuring oxygen partial pressure in fully killed steel melts. Application of HfO_2–ZrO_2–Y_2O_3–Al_2O_3 solid solution for sensor purposes allow to develop an alternative sensor designs with lower consumption of oxide electrolyte materials. In this respect, progress could be made by the plug-type sensor structures combining an alumina insulating tube with the minimised size of the HfO_2–ZrO_2–Y_2O_3–Al_2O_3 pellet.

Acknowledgements

The author wish to thank Professor N. Yamazoe, Dr. K. Shimanoe and Mr. T. Kida (Department of Molecular and Materials Science, Kyushu University, Japan) for their valuable support in preparation of SEM and XRD tests. Furthermore, the author wishes to thank Professor N. Miura for his valuable discussions.

References

1. Chen, I. W. and Chiao, Y. H., Martensite transformations in ZrO_2 and HfO_2 — an assessment of small-particle experiments with metal and ceramic matrices. In *Ceramic Processing Science and Technology*, ed. H. Hausner. American Ceramic Society, Columbos, OH, 1995, pp. 33–45.
2. Janke, D., Oxygen sensing in iron- and steelmaking. In *Ceramic Processing Science and Technology*, ed. H. Hausner. American Ceramic Society, Columbos, OH, 1995, pp. 636–645.
3. Trubelja, M. F. and Stubican, V. S., Phase equilibria and ordering in the system zirconia-hafnia-yttria. *J. Am. Ceram. Soc.*, 1988, **71**(8), 662–666.
4. Shevchenko, A. V., Lopato, L. M., Obolonchik, T. V., Tkachenko, V. D. and Nazarenko, L. V., Liquidus surface for the system HfO_2–ZrO_2–Y_2O_3. *Izv. Acad Nauk SSSR, Neorg. Mater.*, 1987, **23**(3), 452–456.
5. Kim, D. J., Hyun, S. H., Kim, S. G. and Yashima, M., Effective ionic radius of Y^{3+} determined from lattice parameters of fluorite-type HfO_2 and ZrO_2 solid solutions. *J. Am. Ceram. Soc.*, 1994, **77**(2), 597–599.
6. Andrievskaya, E. R. and Lopato, L. M., Phase equiliblia in the system HfO_2–Y_2O_3–CaO. *J. Am. Ceram. Soc.*, 1992, **75**(11), 3026–3032.
7. Trubelja, M. F. and Stubican, V. S., Ionic conductivity of the fluorite-type hafnia-R_2O_3 solid solutions. *J. Am. Ceram. Soc.*, 1991, **74**(10), 2489–2494.
8. Saly, V. and Glushkova, V. B., Electrical behaviour of HfO_2 stabilized with rare earth. *Solid State Ionics*, 1989, **36**, 189–192.
9. Weyl, A. and Janke, D., High-temperature ionic conduction in multicomponent solid oxide solutions based on HfO_2. *J. Am. Ceram. Soc.*, 1996, **79**(8), 2145–2155.
10. Pandit, S. S., Weyl, A. and Janke, D., High-temperature ionic and electronic conduction in zirconate and hafnate compounds. *Solid State Ionics*, 1994, **69**, 93–99.
11. Schieltz, J. D., Patterson, J. W. and Wilder, D. R., Electrolytic behaviour of yttria-stabilised hafnia. *J. Electrochem. Soc.*, 1971, **118**(8), 1257–1261.
12. Kulczycki, A. and Wasiucionek, M., Mechanical and electrical properties of ZrO_2–$6.5Y_2O_3$ ceramic elecrolytes doped with alumina. *Ceramics International*, 1986, **12**, 181–187.
13. Iwase, M., Ichise, E., Takenchi, M. and Yamasaki, T., Measurement of the parameter pe', for the determination of mixed ionic and *n*-type electronic conduction in commercial zirconia electrolytes. *Trans. Jpn Inst. Met.*, 1984, **25**(1), 43–52.
14. Zhuiykov, S., Zirconia single crystal analyser for oxygen measurements. *Process Control and Quality*, 1998, **11**(1), 23–37.
15. Schmalzrid, H., Ionen- und Electronenleitung in Binaren Oxiden und Ihre Untersuching Mittels EMK-Messungen. *Z. Phys. Chem. Neu Folge*, 1963, **38**, 87–102.
16. Lide, D. R., *Handbook of Chemistry and Physics*. CRC Press, Boston, 1996, pp. 5-60–5-63.
17. Vlasov, A. N. and Perfiliev, M. V., Ageing of ZrO_2-based solid electrolytes. *Solid State Ionics*, 1987, **25**, 245–253.
18. Robinson, K., Oxygen probes in heat treatment: a review of current practice and applications. *Heat Treatment of Metals*, 1996, **2**, 43–47.
19. Raeder, H., Norby, T. and Osborn, P. A., Ageing of yttria-stabilized zirconia electrolytes at 1000°C. In *Ceramic Processing Science and Technology*, ed. H. Hausner. American Ceramic Society, Columbos, OH, 1995, pp. 719–723.
20. Blumental, R. N., A tecnical presentation of the factors affecting the accuracy of carbon/oxygen probes. In *Proceeding of the Second Int. Conf. on Carburising and Nitriding with Atmospheres*, Cleveland, 1995, pp. 17–23.